Electronic properties of InN nanowires

Guosheng Cheng,[a] Eric Stern,[a] Daniel Turner-Evans, and Mark A Reed
Departments of Electrical and Biomedical Engineering and Applied Physics, Yale University, P.O. Box 208284, New Haven, Connecticut 06520

(Received 7 September 2005; accepted 25 October 2005; published online 12 December 2005)

Indium nitride nanowires (NWs) grown by a catalyst-free, vapor-solid method are shown to be high-purity, single-crystal hexagonal wurtzite and intrinsic *n* type with uniform diameters that range from 70 to 150 nm and lengths that vary between 3 and 30 μm. Single NWs were fabricated into field-effect transistors and the electronic material parameters of the wires were extracted and are found to be identical to comparable bulk InN. © *2005 American Institute of Physics*.
[DOI: 10.1063/1.2141927]

Semiconducting group-III nitrides have attracted much attention in recent years because of the large gap (0.7–6.2 eV) that can be covered by the nitrides and their alloys.[1–5] In particular, indium nitride (InN) has become the focus of intense research after recent reports of an unexpectedly low band gap of 0.7 eV at room temperature.[6–10] The growth of high quality epitaxial layers of InN has been established by molecular beam epitaxy[11–13] and metalorganic chemical vapor deposition (MCVD).[14–16] However, the fabrication of potential one-dimensional structures, such as nanowires (NWs), has proven difficult due to the thermodynamic properties of In and N. There are reports of InN nanowires syntheses from indium precursors based on the vapor-liquid-solid and the vapor-solid (VS) processes,[17–27] but the mobilities and carrier densities of these NWs have not yet been quantified. In this letter, we discuss a high-yield, catalyst-free method for synthesizing uniform InN NWs and report the fabrication of InN NW field-effect transistors (FETs). Electrical transport results are given for a statistically significant sample, 41 InN NW FETs, across two growth-fabrication runs.

A catalyst-free VS growth strategy was successfully invoked to fabricate InN NWs with yields as large as one gram. A small (1 inch outer diameter), short (3 inch) quartz tube containing a 1:1 ratio of indium:indium oxide powders was loaded in the central region of a hot wall CVD system. The tube was flooded with Ar gas and, while maintaining a base pressure of 1 atm, the temperature was increased. Upon reaching 700 °C the Ar flow was terminated and ammonia was introduced at a rate of 100 sccm and this flow was maintained for 30 min while the temperature was held constant. The furnace was then adiabatically cooled to room temperature in an ammonia atmosphere. This growth procedure repeatably resulted in a large deposition of NW material on the wall of the quartz tube. Lower growth temperatures produced drastically smaller NW yields. Indium nitride NWs extracted from the growth tube were suspended in isopropanol and the suspension was subsequently applied to a glass slide for room-temperature structural and morphological characterization. A representative field-emission scanning electron micrograph (FE-SEM) of the NWs is shown in Fig. 1(a).

In order to fabricate InN NW-FETs, the alcohol suspension was applied dropwise to a Si/SiO_2 wafer with previously defined substrate backgates. This was followed by optical lithography and a liftoff metallization of 50 nm Ni/200 nm Au, which defined unannealed Ohmic contacts to the NWs. The wafer was then surveyed with an automatic device canvassing procedure previously described,[28] and devices were imaged with an FE-SEM to ensure that a unique InN NW contacted lead pairs. A representative device is shown in Fig. 1(b) along with a schematic depicting the FET geometry. An Aglient Technologies 4156B semiconductor parameter analyzer was used to measure $I_{SD}(V_{SD},V_{GD})$. The transconductance is defined as the average of the linear best fits to the positive and negative gate voltage sweeps. The mobility can then be calculated as

$$\mu = \left(\frac{C}{L^2}V_{SD}\right)^{-1} \left.\frac{\partial I_{SD}}{\partial V_{GD}}\right|_{V_{SD}=1.0\ \mathrm{V}}, \quad (1)$$

where $C=2\pi\varepsilon\varepsilon_0 L/\ln(4h/d)$, L is the source-drain length of the NW, h is the SiO_2 thickness, and d is the diameter of the

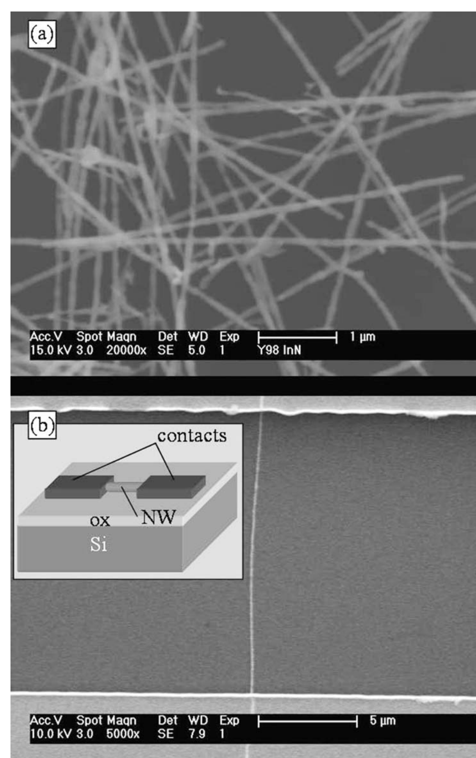

FIG. 1. (a). FE-SEM micrograph of catalyst-free InN nanowires. (b) FE-SEM image of a representative NW device spanning ~14 μm between metal contacts at the top and bottom. The inset shows a schematic of the backgated FET configuration.

[a]Authors to whom correspondence should be addressed; electronic mail: guosheng.cheng@yale.edu, eric.stern@yale.edu

 © 2005 American Institute of Physics
Downloaded 12 Dec 2005 to 128.36.14.184. Redistribution subject to AIP license or copyright, see http://apl.aip.org/apl/copyright.jsp

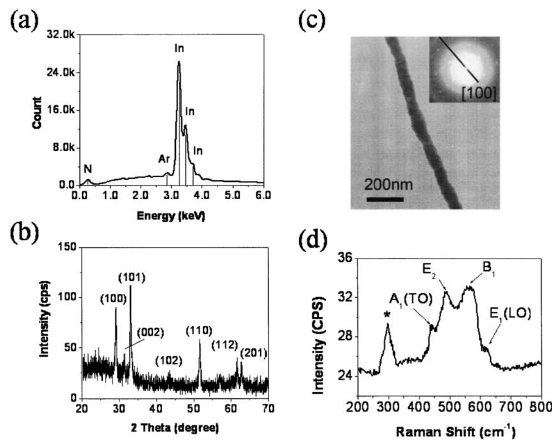

FIG. 2. Structural characterizations of the InN NWs. (a) EDS indicated the presence of In and N in the sample. The Ar is due to the Ar flooding of the growth chamber during temperature ramp-up. (b) XRD spectrum corresponding to hexagonal wurtzite InN nanowires. (c) TEM image with electron diffraction pattern (inset). (d) Micro-Raman spectroscopy of wurtzite InN NWs and the indexed active modes at room temperature. The peak with asterisk "*" denotes zone-boundary phonon of wurtzite InN.

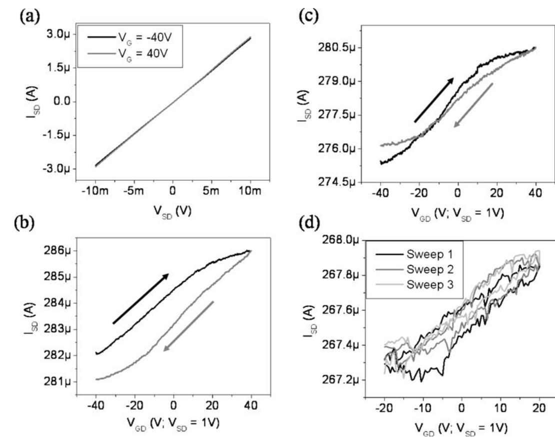

FIG. 3. (a) Near-zero bias $I_{SD}(V_{SD})$ plot for $V_{GD}=-40$ (black) and 40 V (gray) for a representative device illustrating Ohmic behavior. (b) $I_{SD}(V_{GD})$ dependence at $V_{SD}=1$ V for the same device from (a). The −40–40 V sweep is taken first, as indicated by the arrows. The forward transconductance is 19.6% smaller than the reverse, the greatest disparity of the 41 devices reported in this study. (c) $I_{SD}(V_{GD})$ dependence at $V_{SD}=1$ V for a typical sample. Again, the sweep order is indicated by the arrows. (d) Multiple $I_{SD}(V_{GD})$ measurements at $V_{SD}=1$ V for a third device. V_{GD} is swept from −20 to 20 V. Sweep 1 is the initial sweep, sweep 2 is an instantaneous subsequent sweep, and sweep 3 is a subsequent sweep taken after a 5 min lag.

NW. The carrier density is then determined by

$$n=\frac{\sigma}{e\mu}. \tag{2}$$

Nanowire lengths were measured to the nearest 0.05 μm and diameters to 5 nm. For the 41 samples reported here, the average diameter is 113±4 nm (standard error of the mean). For variable-temperature measurements the wafers were diced, wirebonded, and measured in a variable temperature helium-flow cryostat.

SEM micrographs revealed NW lengths ranging from 3 to 30 μm and diameters from 70 to 150 nm (although individual NWs were uniform to within 15 nm). Nanobelts were also observed, but in minute numbers. Energy dispersive spectroscopy (EDS) [Fig. 2(a)] indicates the sole presence of In and N in the sample (the Ar signal is an experimental artifact). X-ray diffraction (XRD) [Fig. 2(b)] indexes the NWs as hexagonal wurtzite with primitive cell parameters: $a=3.536$ Å and $c=5.709$ Å. The reflection peaks were indexed (100), (002), (101), (102), (110), (112), and (201), corresponding to wurtzite InN. A transmission electron micrograph (TEM) with its accompanying diffraction pattern illustrates that although there is some surface roughness, the NW is single crystal with growth along [100] [Fig. 2(c)]. The micro-Raman spectrum (300 K) also corresponds to single-crystal wurtzite InN. In Fig. 2(d), the four active modes A_1 (TO) (444 cm^{-1}), E_2 (high) (490 cm^{-1}), B_1 (566 cm^{-1}), and E_1 (LO) (619 cm^{-1}) of hexagonal wurtzite InN are observed. One additional mode at ~299 cm^{-1} is present, possibly due to the zone-boundary phonon activated by the finite-size effects.[29,30]

Two separate growth and processing runs yielded 41 well-behaved devices; though there were no discernable physical differences between the ~120 total devices measured, approximately 2/3 exhibited spurious charging effects—including specious *p*-type behavior—indicative of parasitic defects, and were excluded.

All devices discussed this study had Ohmic contacts, as illustrated in the near-zero bias characteristics of Fig. 3(a), with linear best-fit R^2 values of 0.99 or greater (for all temperatures measured). The devices had resistivities of $\sim 4\times10^{-4}$ Ω cm, similar to those observed in earlier measurements for catalyst-grown single-crystal InN NWs with similar diameters.[24] We note that NWs of the higher resistivities (similar to those reported in Ref. 23) do not show well-behaved FET behavior for these samples.

$I_{SD}(V_{GD})$ plots of the well-behaved FET devices are shown in Figs. 3(b)–3(d). Figure 3(b) illustrates the generic behavior, e.g., I_{SD} increasing monotonically with increasing V_{GD} (likewise, decreasing monotonically with decreasing V_{GD}) indicative of *n*-type material, as seen in bulk InN.[30] Some degree of hysteresis due to a fixed charge trap distribution is observed in all devices; Fig. 3(c) is typical, whereas Fig. 3(b) [Fig. 3(d)] illustrated the worst [best] hysteresis. Transconductances are calculated as the average of the linear best fits to the forward and reverse V_{GD} sweeps and there was found to be no correlation between the degree of hysteresis and transconductance. Additionally, Fig. 3(d) illustrates charge trapping dynamics are unimportant for these measurement conditions. The average transconductance is $2.24\pm0.39\times10^{-8}$ A/V, similar to that seen previously for GaN NW samples.[31]

Mobilities and carrier densities of the 41 NW devices (26 from the first run and 15 from the second) are plotted in Fig. 4(a). The InN NWs had an average mobility of 29.2±5.4 (standard error of the mean, σ_{SEM}) cm^2/V s, and an average carrier density of $1.83\pm0.38(\sigma_{SEM})\times10^{21}$ cm^{-3}. A decreasing trend of mobility with increasing doping density is observed, similar to that seen for InN grown epitaxially on sapphire[32] and GaN (Refs. 32–35) substrates. The results show that the quality of the InN NW material grown by the VS CVD technique is comparable to bulk epitaxial material, though the intrinsic carrier density is larger [presumably due to N vacancies, as for bulk InN (Ref. 36) and GaN NWs (Ref. 31)].

The temperature dependence of the mobility [Fig. 4(b)] was investigated for two randomly selected samples with

Downloaded 12 Dec 2005 to 128.36.14.184. Redistribution subject to AIP license or copyright, see http://apl.aip.org/apl/copyright.jsp

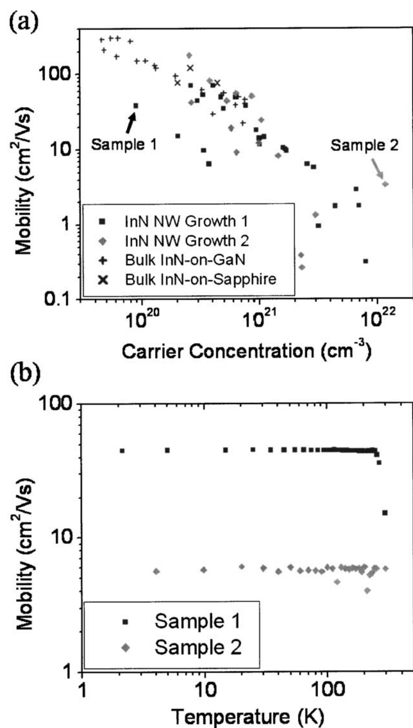

FIG. 4. (a) Scatter plot of mobility vs log carrier concentration for two growth-fabrication runs of InN NWs. There are a total of 41 NW samples plotted, 26 from the first run and 15 from the second run. Data from bulk epitaxially grown InN on sapphire (see Ref. 32) and GaN (see Refs. 32–35) substrates are included. The datapoints from samples used for temperature-dependence measurements are arrowed and labeled. (b) Temperature dependence of mobility for two InN NW samples. Sample 1 has a carrier concentration of 8.96×10^{19} cm^{-3} and sample 2 of 1.16×10^{22} cm^{-3}.

roughly two orders of magnitude different carrier densities—8.96×10^{19} cm^{-3} for sample 1, and 1.16×10^{22} cm^{-3} for sample 2—and each with a hysteresis similar to that of Fig. 3(c). Both samples exhibit essentially temperature-independent mobilities, although the higher-mobility sample exhibited a high temperature roll-off and a very weak ($\sim 2\%$) low-temperature metallic behavior. Further investigation is necessary to elucidate the mechanisms responsible for these dependencies.

This study demonstrates that catalyst-free, single-crystal InN NWs have comparable electron mobilities to bulk epitaxial InN, thus providing a system whereby one can separate contributions of material from dimensionality or other NW effects (such as defect incorporation). The statistically significant study presented here shows that intrinsic material parameters can be quantified even in the presence of a large percentage of defect-dominated devices.

The authors would like to thank Stan Guthrie for assistance with fabrication, Professor Jung Han, Dr. Michael Young, and Dr. James Hyland for many helpful discussions, Dr. Elena Cimpoiasu, Ryan Munden, and Aric Sanders for aiding with the measurement setup, and Dr. Zhenting Jiang for help with FE-SEM microscopy. This work was partially supported by DARPA through AFOSR, ARO (DAAD19-01-1-0592), AFOSR (F49620-01-1-0358), NASA (NCC 2-1363), by the Department of Homeland Security, and by the National Science Foundation.

[1]S. Nakamura, T. Mukai, and H. M. Seno, Appl. Phys. Lett. **64**, 1687 (1994).
[2]S. Nakamura, Science **281**, 956 (1998).
[3]S. Strife and H. Morkoc, J. Vac. Sci. Technol. B **10**, 1237 (1992).
[4]I. Vurgaftman, J. R. Meyer, and L. R. Ram-Mohan, J. Appl. Phys. **89**, 5815 (2001).
[5]D. Zhuang and J. H. Edgar, Mater. Sci. Eng., R. **48**, 1 (2005).
[6]K. S. A. Butcher and T. L. Tansley, Superlattices Microstruct. **38**, 1 (2005).
[7]Z. G. Qian, W. Z. Shen, H. Ogawa, and Q. X. Guo, J. Phys.: Condens. Matter **16**, R381 (2004).
[8]Q. X. Guo, T. Tanaka, and M. Nishio, Appl. Phys. Lett. **86**, 231913 (2005).
[9]H. L. Xiao, X. L. Wang, J. X. Wang, N. H. Zhang, H. X. Liu, Y. P. Zeng, J. M. Li, and Z. G. Wang, J. Cryst. Growth **276**, 401 (2005).
[10]K. M. Yu, Z. Liliental-Weber, W. Walukiewicz, W. Shan, J. W. Ager, S. X. Li, R. E. Jones, E. E. Haller, H. Lu, and W. J. Schaff, Appl. Phys. Lett. **86**, 071910 (2005).
[11]E. Tiras, D. Zanato, S. Mazzucato, N. Balkan, and W. J. Schaff, Superlattices Microstruct. **36**, 473 (2004).
[12]Y. Saito, N. Teraguchi, A. Suzuki, T. Araki, and Y. Nanishi, Jpn. J. Appl. Phys., Part 2 **40**, L91 (2001).
[13]H. Lu, W. J. Schaff, J. Hwang, H. Wu, G. Koley, and L. F. Eastman, Appl. Phys. Lett. **79**, 1489 (2001).
[14]Y. Huang, H. Wang, Q. Sun, J. Chen, D. Y. Li, Y. T. Wang, and H. Yang, J. Cryst. Growth **276**, 13 (2005).
[15]D. A. Neumayer and J. G. Ekerdt, Chem. Mater. **8**, 9 (1996).
[16]A. Yamamoto, M. Tsujino, M. Ohkubo, and A. Hashimoto, J. Cryst. Growth **137**, 415 (1994).
[17]S. Vaddiraju, A. Mohite, A. Chin, M. Meyyappan, G. Sumanasekera, B. W. Alphenaar, and M. K. Sunkara, Nano Lett. **5**, 1625 (2005).
[18]L. W. Yin, Y. Bando, D. Golberg, and M. S. Li, Adv. Mater. (Weinheim, Ger.) **16**, 1833 (2004).
[19]M. C. Johnson, C. J. Lee, E. D. Bourret-Courchesne, S. L. Konsek, S. Aloni, W. Q. Han, and A. Zettl, Appl. Phys. Lett. **85**, 5670 (2004).
[20]C. H. Liang, L. C. Chen, J. S. Hwang, K. H. Chen, Y. T. Hung, and Y. F. Chen, Appl. Phys. Lett. **81**, 22 (2002).
[21]Z. H. Lan, W. M. Wang, C. L. Sun, S. C. Shi, C. W. Hsu, T. T. Chen, K. H. Chen, C. C. Chen, Y. F. Chen, and L. C. Chen, J. Cryst. Growth **269**, 87 (2004).
[22]J. Zhang, B. L. Xu, F. H. Jiang, Y. D. Yang, and J. P. Li, Phys. Lett. A **337**, 121 (2005).
[23]T. Tang, S. Han, W. Jin, X. L. Liu, C. Li, D. H. Zhang, C. W. Zhou, B. Chen, J. Han, and M. Meyyapan, J. Mater. Res. **19**, 423 (2004).
[24]C. Y. Chang, G. C. Chi, W. M. Wang, L. C. Chen, K. H. Chen, F. Ren, and S. J. Pearton, Appl. Phys. Lett. **87**, 093112 (2005).
[25]J. Zhang, L. Zhang, X. Peng, and X. Wang, J. Mater. Chem. **12**, 802 (2002).
[26]K. Sardar, F. L. Deepak, A. Govindaraj, M. M. Seikh, and C. N. R. Rao, Small **1**, 91 (2004).
[27]B. Schwenzer, L. Loeffler, R. Seshardri, S. Keller, F. F. Lange, S. P. DenBaars, and U. K. Mishra, J. Mater. Chem. **14**, 637 (2004).
[28]E. Stern, G. Cheng, C. Li, J. Klemic, E. Broomfield, D. Turner-Evans, C. Zhou, and M. A. Reed, J. Vac. Sci. Technol. B (to be published).
[29]M. Kuball, J. W. Pomeroy, M. Wintrebert-Fouquet, K. S. A. Butcher, H. Lu, and W. J. Schaff, J. Cryst. Growth **269**, 59 (2004).
[30]A. G. Bhuiyan, A. Hashimoto, and A. Yamamoto, J. Appl. Phys. **94**, 2779 (2003).
[31]E. Stern, G. Cheng, E. Cimpoiasu, R. Klie, S. Guthrie, J. F. Klemic, I. Kretzschmar, E. Steinlauf, D. Turner-Evans, E. Broomfield, J. Hyland, R. Koudelka, T. Boone, M. Young, A. Sanders, R. Munden, T. Lee, D. Routenberg, and M. A. Reed, Nanotechnology (to be published).
[32]A. Yamamoto, T. Shin-Ya, T. Sugiura, and A. Hashimoto, J. Cryst. Growth **189/190**, 461 (1998).
[33]C. R. Abernathy, S. J. Pearton, R. Ren, and P. W. Wisk, J. Vac. Sci. Technol. B **11**, 179 (1993).
[34]W. A. Bryden, S. A. Ecelberger, and T. J. Kistenmacher, Appl. Phys. Lett. **64**, 2864 (1994).
[35]Y. Sato and S. Sato, J. Cryst. Growth **146**, 262 (1994).
[36]T. L. Tansley and C. P. Foley, Electron. Lett. **20**, 1066 (1984).

Downloaded 12 Dec 2005 to 128.36.14.184. Redistribution subject to AIP license or copyright, see http://apl.aip.org/apl/copyright.jsp